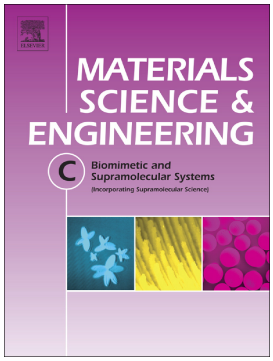

Graphene oxide modified single-use electrodes and their application for voltammetric miRNA analysis

Deniz Isin, Ece Eksin, Arzum Erdem

PII: S0928-4931(16)32298-6
DOI: doi: 10.1016/j.msec.2017.02.166
Reference: MSC 7500

To appear in: *Materials Science & Engineering C*

Received date: 21 November 2016
Revised date: 24 February 2017
Accepted date: 28 February 2017

Please cite this article as: Deniz Isin, Ece Eksin, Arzum Erdem , Graphene oxide modified single-use electrodes and their application for voltammetric miRNA analysis. The address for the corresponding author was captured as affiliation for all authors. Please check if appropriate. Msc(2017), doi: 10.1016/j.msec.2017.02.166

Graphene oxide modified single-use electrodes and their application for voltammetric miRNA analysis

Deniz Isin, Ece Eksin and Arzum Erdem*

Faculty of Pharmacy, Analytical Chemistry Department, Ege University, 35100 Bornova, Izmir, TURKEY

**** Corresponding author:(A. Erdem)***
E-mail: arzum.erdem@ege.edu.tr and arzume@hotmail.com
Phone: + 90-232-3115131

Abstract

The modification of graphene oxide (GO) onto the surfaces of chemically activated pencil graphite electrodes (PGEs) were performed herein, and then these electrodes were applied for the first time on voltammetric monitoring of miRNAs. The specific recognition of miRNA-34a, which has been related to Alzheimer disease, was explored in the presence of DNA-RNA hybridization by using CA/GO/PGEs in combination with differential pulse voltammetry (DPV) technique. The characterization of CA/GO/PGE was investigated by cyclic voltammetry (CV), electrochemical impedance spectroscopy (EIS), and scanning electron microscopy (SEM). The effect of GO concentration, DNA probe concentration and miRNA-34a concentration upon to biosensor response was optimized, and accordingly, the selectivity of miRNA-34a biosensor was tested under the optimum conditions.

Keywords: Graphene oxide; miRNA; pencil graphite electrode; differential pulse voltammetry; electrochemical biosensor; Alzheimer disease

1. Introduction

Graphene is a rapidly rising star on the horizon of materials science and it's a two-dimensional (2D) sheet composed of sp^2-bonded single-layer carbon atoms with the honeycomb lattice structure. The graphene oxide (GO), derives its name from the oxidation process of graphite, and are known to be extensively researched materials. Graphene and graphene-based materials have been attracting great research interest because of their unique structural features; high surface area, flexibility, perfect electric and thermal conductivity, and chemical stability [1-3]. Due to its fast electron mobility, high specific surface area, quantum Hall effect, and upstanding electric conductivity, graphene is becoming an ideal material for the construction of biosensors for nucleic acid hybridization, protein electrochemistry, and small-molecule detection [4-12].

The one of advantages of the graphene oxide is its easy dispersibility in water and other organic solvents, as well as in different matrixes, due to the presence of the oxygen functionalities. It remains as a very important property when mixing the material with ceramic or polymer matrixes for trying to improve their electrical and mechanical properties [13].

microRNAs (miRNAs) are potentially useful biomarkers for early diagnosis of numerous human diseases [14]. Their aberrant expression could be associated with cancer development and a variety of diseases. Increasing evidence has revealed that aberrant miRNA expression level in the blood and cell samples is associated with various human diseases such as cancer and cardiovascular diseases [15]. Physiologic concentrations of mature and precursor forms of miRNA vary depending on species, tissue, cell type and disease state with ranges from nanomolar to fetamolar concentrations [16]. Recent studies have identified the role of miRNAs in regulating key cellular processes and signaling pathways involved in tumourigenesis, including cell proliferation, differentiation, angiogenesis, apoptosis,

invasion and metastasis. miR-34a is a tumor suppressive miRNA across many tumor types through its ability to inhibit cellular proliferation, invasion and tumor sphere formation. miR-34a also shows promise within certain in vivo solid tumor models [17].

Accurate and efficient detection of miRNAs in clinical samples is still challenging because of their short and highly homologous sequences and low concentrations [18, 19]. Several modern techniques have been developed for miRNA analysis, including electrochemistry [20-26], fluorescence [27], electrochemiluminescence [28], and Surface Plasmon Resonance (SPR) [29] etc. Electrochemical detection offers advantages as an alternative to conventional methods due to its wide detection range, short time consumption, tendency to miniaturization, high sensitivity and selectivity [30]. Currently, the studies have been progressed in order to develop sensitive electrochemical biosensors for the sensitive detection of low-abundance miRNAs [15, 22-26, 30-44].

To our best knowledge, this is the first study in the literature, which presented the label free voltammetric detection of miRNA-34a by using CA/GO modified PGEs. Under this goal, the modification of graphene oxide (GO) onto the surfaces of chemically activated pencil graphite electrodes (PGEs) was firstly performed in our study, and then these electrodes were applied on voltammetric monitoring of miRNAs based on the changes at guanine oxidation signal. The characterization of each electrode; PGE, CA/PGE, GO/PGE and CA/GO/PGEs was investigated by cyclic voltammetry (CV), electrochemical impedance spectroscopy (EIS), and scanning electron microscopy (SEM) techniques. The electrochemical detection of specific recognition of miRNA-34a was performed in full match DNA-miRNA hybridization using CA/GO/PGEs in combination with differential pulse voltammetry (DPV) technique. The effect of GO concentration, DNA probe concentration, miRNA-34a concentration upon to biosensor response was also investigated. Under the

optimum experimental conditions, the sequence-selective DNA hybridization related to miRNA-34a was explored in the case of hybridization between miRNA-34a probe and its complementary RNA target, or non-complementary (NC), or in the presence of mixture sample containing miRNA-34a target and non-complementary miRNA (1:1).

2. Experimental Procedure

2.1. Apparatus

DPV measurements were performed on a µ-AUTOLAB system and a GPES 4.9 software package (Eco Chemie, The Netherlands). The raw data were treated using the Savitzky and Golay fillter (level 2) of the GPES software, followed by the moving average baseline correction with a peak width of 0.03.

CV and DPV measurements were performed with a traditional three-electrode system using a disposable pencil graphite electrode (PGE), a platinum wire and an Ag/AgCl/KCl/3M (BAS, Model RE-5B, W. Lafayette, USA) as working, counter and reference electrode, respectively. All measurements were performed in a Faraday cage (Eco Chemie, The Netherlands).

2.2. Chemicals

Graphene oxide (GO) was purchased from DropSens (Spain). The chemical linkers used for covalent attachment; N-hydroxysuccinimide (NHC) and N-(3-dimethylaminopropyl)-N'-ethylcarbodiimide hydro-chloride (EDC) were purchased from Sigma-Aldrich.

Other chemicals were in analytical reagent grade and they were supplied from Sigma and Merck.

The amino linked miRNA-34a specific DNA probe, miRNA-34a RNA target (i.e, the complementary of miRNA-34a specific DNA probe), and other miRNA sequences were purchased from Ella Biotech (Germany) as lyophilized powder. The base sequences of miRNAs are listed below:

miRNA-34a G specific DNA probe: (miRNA-34a G probe)

5'-NH_2- $(CH_2)_6$ - ACA ACC AGC TAA GAC ACT GCC A-3'

Inosine substituted miRNA-34a specific DNA probe: (miRNA-34a I probe)

5'-NH_2- $(CH_2)_6$- ACA ACC AXC TAA XAC ACT XCC A- 3' (X= Inosin)

miRNA-34a RNA target:

5' -UGG CAG UGU CUU AGC UGG UUG U-3' (U=Urasil)

Non-complementary (NC) miRNAs:

miRNA-15a:

5'-UAG CAG CAC AUA AUG GUU UGU G-3'

miRNA-16:

5'-UAG CAG CAC GUA AAU AUU GGC G-3'

miRNA-155:

5'-UUA AUG CUA AUC GUG AUA GGG GU-3'

miRNA-660:

5'-UAC CCA UUG CAU AUC GGA GUU G-3'

All miRNA stock solutions (500 µg/mL) were prepared with Tris–EDTA buffer (10 mM Tris–HCl, 1 mM EDTA, pH 8.0; TE) and kept frozen. More diluted solutions of miRNAs were prepared with 50 mM phosphate buffer containing 20 mM NaCl (PBS, pH 7.4).

Ultra-pure water was used in order to prepare all aqueous solutions.

2.3. Procedure

The procedure included ***(i)*** chemical activation of PGE surface using covalent agents (CA) ***(ii)*** GO modification onto CA-PGE surfaces, ***(iii)*** immobilization of miRNA-34a specific DNA probe onto CA/GO/PGE surface, ***(iv)*** hybridization of miRNA-34a specific DNA probe with miRNA-34a RNA target, or non-complementary RNAs (miRNA-15a/miRNA-16/miRNA-155/miRNA-660) at CA/GO modified electrode surface.

PGE surface activation and hybridization processes were carried out at + 4 ^{o}C. Other experiments were done at room temperature. The experimental procedure was presented in Figure 1.

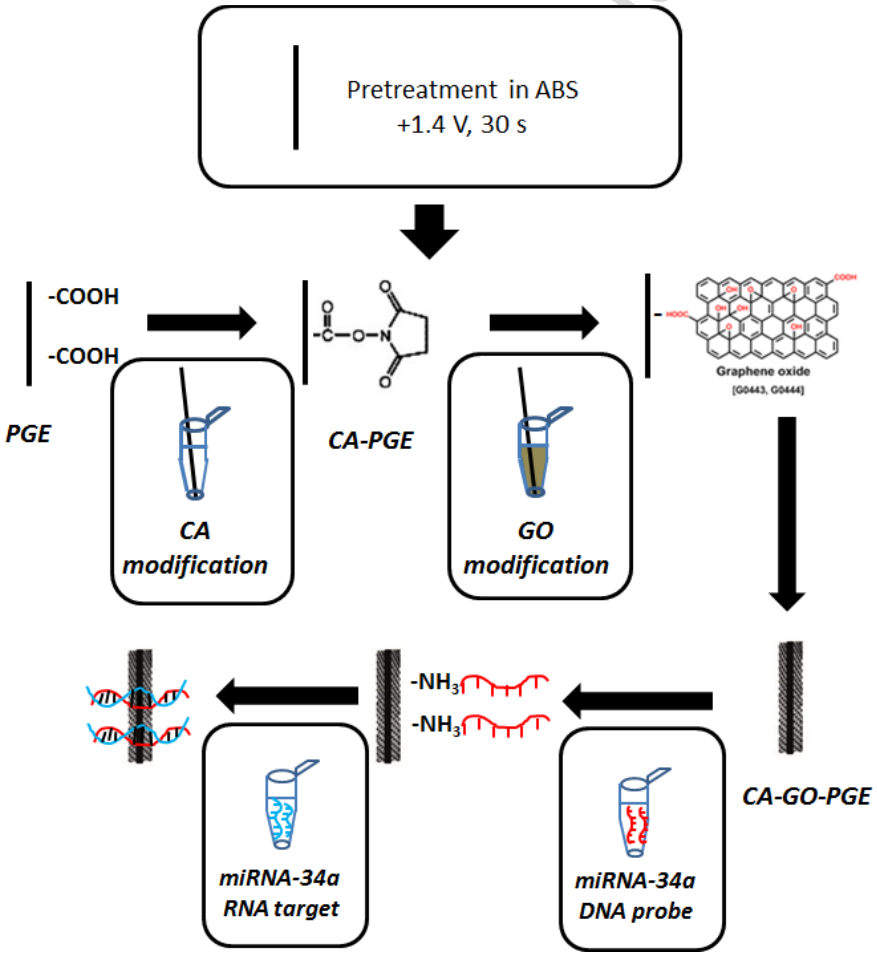

Fig. 1. The representative scheme of experimental procedure followed in the hybridization occured between miRNA-34a target and its complementary DNA probe at the surface of CA/GO/PGEs.

2.3.1. Preparation of CA solution and chemical activation of PGE surfaces

The CA solution was prepared by 5 mM EDC and 5 mM NHS prepared in phosphate buffer solution (PBS, pH 7.4). PGEs were electrochemically pretreated by applying a potential of +1.40 V for 30 s in 0.5 M acetate buffer containing 20 mM NaCl (ABS, pH 4.8) [12, 24,25]. Each pretreated PGE was immersed into the vials containing 100 µL of 5 mM CA solution during 1 hour to obtain activated carboxyl groups at the surface of PGEs before GO modification. N-Hydroxysuccinimide (NHS) is an organic compound and after its mixing with a coupling reagent such as N-(3-dimethylaminopropyl)-N'-ethylcarbodiimide hydro-chloride (EDC), a highly reactive activated acid intermediate (CA) could be formed. It has been reported earlier that CA modification stabilizes the surfaces of electrodes and it also provides better attachment for GO onto surface [45].

2.3.2. Preparation of GO solution and GO modified PGEs

The required amount of GO was suspended in dimethyl sulfoxide (DMSO) and sonicated during 1 hour. Each of chemically activated pencil graphite electrodes (PGEs) was immersed into the vials containing 100 µL of GO solution for 15 minute for easy surface modification of PGEs [25]. Each of the CA/GO/PGEs was then allowed to dry for 5 min in an upward position.

2.3.3. Immobilization of microRNA-34a specific DNA probe onto the surface of CA/GO/PGEs

The required amount of miRNA-34a specific DNA probe was prepared in PBS (pH 7.4). Each of CA/GO/PGEs was immersed into the vials containing miRNA-34a solution and immobilization was then carried out at + 4 ^{o}C during 60 min. Each of the electrodes was then rinsed with PBS for 10 s to remove unbound probe from electrode surface.

2.3.4. DNA-RNA hybridization at the surface of probe immobilized CA/GO/PGE

miRNA-34a DNA probe immobilized electrodes were immersed into the vials containing 35 µg/mL target miRNA prepared in PBS (pH 7.4) for hybridization process and the electrodes were kept for an hour. Each of the modified electrodes was then rinsed with PBS for 10 s.

2.3.5. Voltammetric Measurements

CV measurements were performed in potential range from −0.8 to +1.45 V with the scan rate as 50 mV/s in a redox probe solution of 2 mM $K_3[Fe(CN)_6]/K_4[Fe(CN)_6]$ (1:1) prepared in 0.1 M KCl.

DPV measurements were performed in ABS (pH 4.80) for electrochemical detection of hybridization between miRNA-34a DNA probe and miRNA-34a target. The chemical mechanism of the oxidation of guanine has been used to detect the hybridization of miRNA on the electrode surface, because guanine is the most redox active nitrogenous base in DNA [23, 24,26, 46, 47]. The guanine oxidation signal was then measured between the potential of +0.2 V and +1.40 V with a pulse amplitude of 50 mV and a scan rate of 50 mV/s.

3. Results and discussion

The microscopic characterization of disposable graphite electrodes; unmodified PGE, CA/PGE and CA/GO/PGEs was performed via SEM and given in Figure 2. After activation of the PGE surface by CA, due to the film layer at the CA modified electrode surface (Fig. 2 c,d), there is more bright surface in contrast to the unmodified one (Fig. 2 a,b). It was clearly shown that the PGE surface was more stratified after GO modification onto the surfaces of CA/PGEs (Fig. 2 g,h) in contrast to the ones of GO/PGEs in the absence of CA (Fig. 2 e,f). According to the images given at Fig. 2 g,h, it can be concluded that the surfaces of CA/PGEs was successfully modified by using GO.

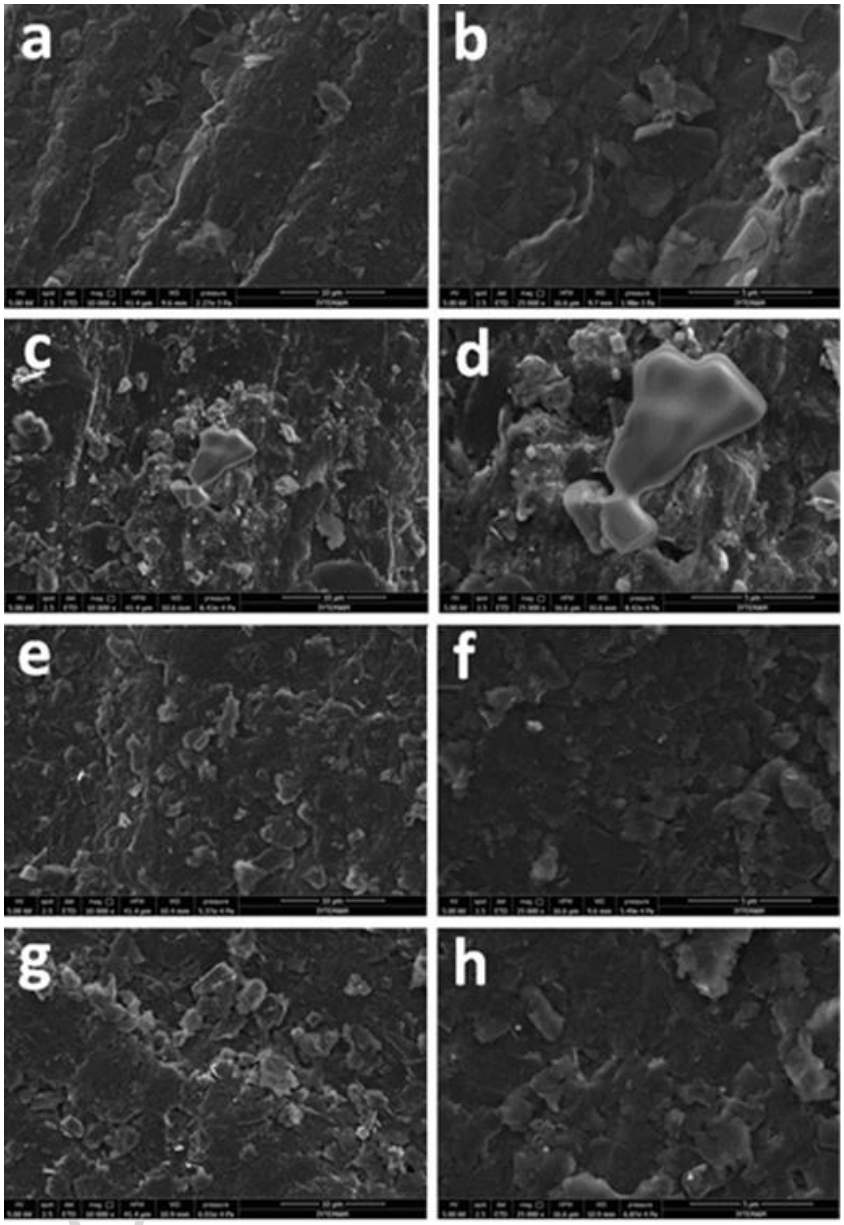

Fig. 2. SEM images of (a,b) unmodified PGE, (c,d) CA modified PGE, (e,f) GO modified PGE, (g,h) CA and GO modified PGE (CA/GO/PGE) respectively with resolution at 10 µm and 1µm.

Next, the effect of GO concentration upon the biosensor response was investigated (Fig. 3). The modification of GO in different concentrations onto the surface of PGE was performed and then, CV measurements were done. The average anodic peak current (I_a) was measured as 73.3 ± 12.7 µA with the relative standard deviation % (RSD %) as 13.2% (n = 10) using PGEs. After the modification of

200 µg/mL, 400 µg/mL and 600 µg/mL GO onto the surface of CA/PGEs, the average I_a was obtained as 78.3 ± 12.7 µA, 99.2 ± 12.7 µA and 94.8 ± 3.9 µA with the RSDs % as 16.2%, 4.5% and 4.1% (n = 4) respectively. The increase ratio % at I_a from CA-PGE to CA/GO/PGE was calculated and found as 36%, 87%, 49%, respectively, after the modification of 200 µg/mL, 400 µg/mL and 600 µg/mL GO onto the surface of CA/PGEs. Due to the conductive structure of GO [48, 49], there was an increase at I_a in the presence of GO modification onto electrode surface. According to these results, it was concluded that the surfaces of 400 µg/mL GO modified PGEs became the most conductive ones of all. Therefore, 400 µg/mL GO concentration was chosen as the optimum GO concentration for our further experiments.

The highest Q_a was obtained after modification of 400 µg/mL GO onto the surface of CA/PGE. According to the value of peak to peak separations (ΔE_p), the highest decrease was determined by unmodified PGE (ΔE_p = 0.129 V) and CA/PGE (ΔE_p = 0.148 V) to CA/GO/PGE after 400 µg/mL GO modification onto CA/PGE (200 µg/mL GO modification; ΔE_p = 0.105 V, 400 µg/mL GO modification; ΔE_p = 0.095, 600 µg/mL GO modification; ΔE_p = 0.125 V). This result indicated that the modification of GO onto PGE surface made the behavior of $[Fe(CN)_6]^{3-/4-}$ less irreversible [5, 50].

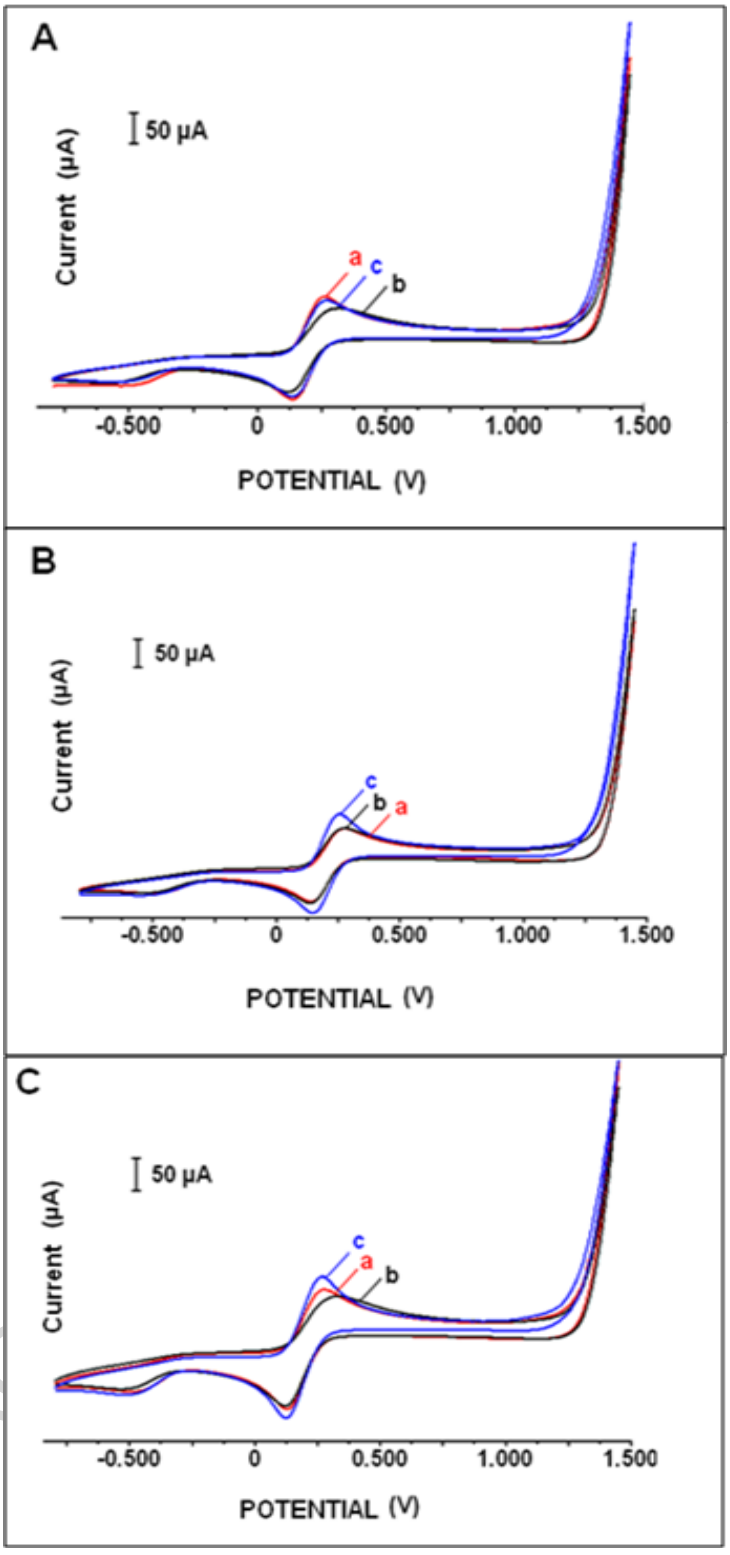

Fig. 3. (A) Cyclic voltammograms of **(A) (a)** unmodified PGE, **(b)** CA/PGE, **(c)** 200 µg/mL GO modified CA/PGE, **(B) (a)** unmodified PGE**,** **(b)** CA/PGE, **(c)** 400 µg/mL GO modified CA/PGE, **(C) (a)** unmodified PGE, **(b)** CA/PGE, **(c)** 600 µg/mL GO modified CA/PGE.

The characterization of PGE, CA/PGE and 400 µg/mL GO modified CA/PGE was performed using cyclic voltammetry to present the advantages of CA activation and GO modification onto PGE surface.

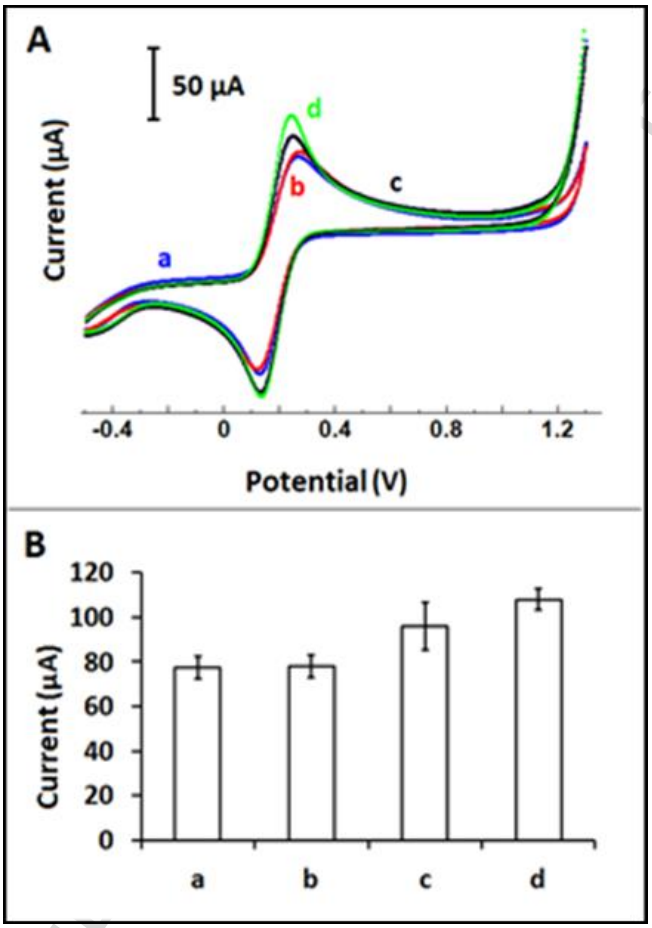

Fig. 4. (A) Voltammograms presenting the signals obtained by **(a)** unmodified PGE, **(b)** CA/PGE, **(c)** GO/PGE, **(d)** GO modified CA activated PGE (CA/GO/PGE). **(B)** Histograms representing the average anodic peak currents (n=3) of **(a)** unmodified PGE, **(b)** CA/PGE, **(c)** GO/PGE, **(d)** CA/GO/PGE.

According to the CV measurements; average anodic peak currents (Ia), anodic charge values (Qa) and calculated surface areas (A) of PGE, CA/PGE, GO/PGE and CA/GO/PGEs were shown in Table 1.

Table 1. Average anodic peak currents (I_a), anodic charge values (Q_a) and calculated surface areas (A) of PGE, CA/PGE, 400 µg/mL GO modified PGE and 400 µg/mL GO modified CA/PGE (n=3).

	I_a (µA)	Q_a ($C*10^{-4}$)	A (cm^2)
PGE	77.3 ± 5.0	13.1 ± 0.3	0.23
CA/PGE	78.0 ± 4.9	14.2 ± 0.4	0.24
GO/PGE	95.9 ± 10.6	16.4 ± 0.9	0.28
CA/GO/PGE	108.0 ± 4.5	17.2 ± 0.9	0.33

After GO modification onto CA/PGE surface, an increase at anodic peak current was determined about 38.5 % (Fig. 4). Additionally, the largest surface area as 0.33 cm^2 was obtained by CA/GO/PGE in contrast to the ones of PGE, CA/PGE and GO/PGE. This result was a proof that the electroactive surface area of CA/GO/PGE increased in comparison to the CA/PGE due to the layered structure of GO, similarly to earlier works [51-53].

The impedimetric surface characterization of PGE, CA/PGE and 400 µg/mL GO modified CA/PGE was then performed by electrochemical impedance spectroscopy (EIS) technique to present the advantages of CA activation and GO modification onto PGE surface (Figure 5). The average R_{ct} values of unmodified PGE, CA/PGE and CA/GO/PGE were measured as 110.2 ± 45.5 Ohm (RSD %, 41.3 %, n=3), 225.8 ± 74.4 Ohm (RSD %, 32.9 %, n=3) and 56.7 ± 18.7 Ohm (RSD %, 32.9 %, n=3) After GO modification onto CA/PGE surface, 74.9 % decrease at R_{ct} was recorded (Fig 5- b to c). This decrease proved that GO modification yield an increase at the conductivity of PGE surface since there is an increase at the interfacial electron transfer performed between the electrode and the electroactive species in solution [12, 25,48].

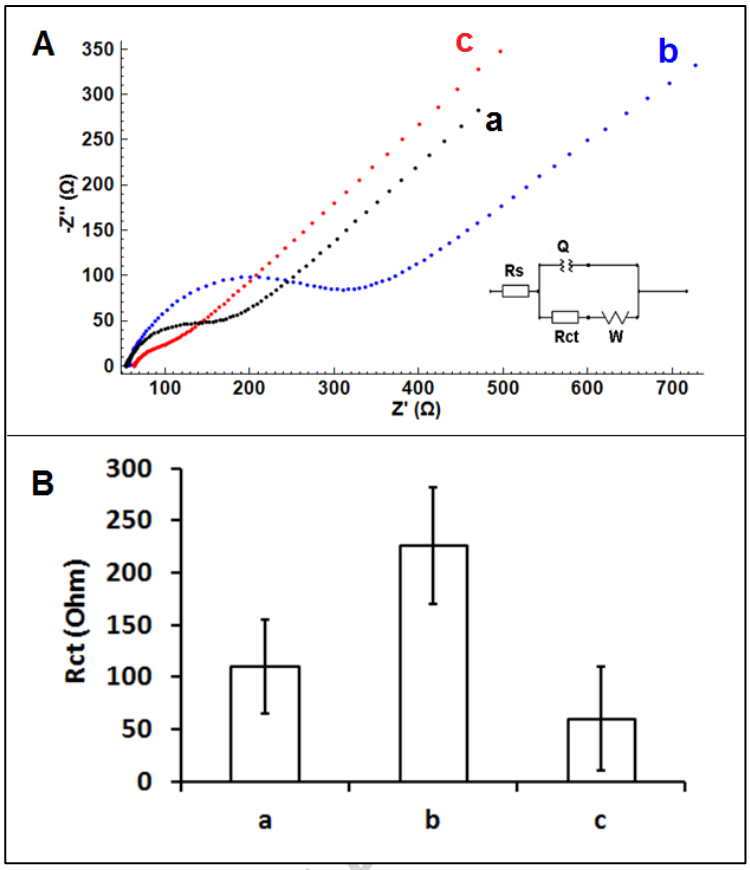

Figure 5. (A) Nyquist diagrams of (a) PGE, (b) CA/PGE, (c) CA/GO/PGE in 2,5 mM $Fe(CN)_6^{3-/4-}$. (B) Histograms representing the average R_{ct} values of (a) PGE, (b) CA/PGE, (c) CA/GO/PGE's (n=3). Inset was the equivalent electrical model used to fit the impedance data, the parameters of which are listed in the text; R_S is the solution resistance. The constant phase element Q is then related to the double layer capacitance at the electrode-electrolyte interface. R_{ct} is related to the charge transfer resistance at the electrode-electrolyte interface. The constant phase element W is the Warburg impedance due to mass transfer to the electrode surface.

The effect of miRNA-34a G DNA probe concentration upon to biosensor response was investigated by using unmodified, CA modified and CA/GO modified PGEs (Fig.6). Amino linked miRNA-34a at the concentration level ranging from 5 to 15 µg/mL was immobilized and the increase ratio % at the guanine signal measured by CA/GO/PGEs was calculated in contrast to the CA/PGEs. A gradual

increase was recorded at guanine signal by CA/GO/PGEs till 10 µg/mL, and then it leveled off. The average guanine signal was measured as 1846 ± 318.9 nA (RSD% = 17.3%, n = 2) after the immobilization of 10 µg/mL miRNA-34a G probe at CA/GO/PGEs (Fig. 6B-g).

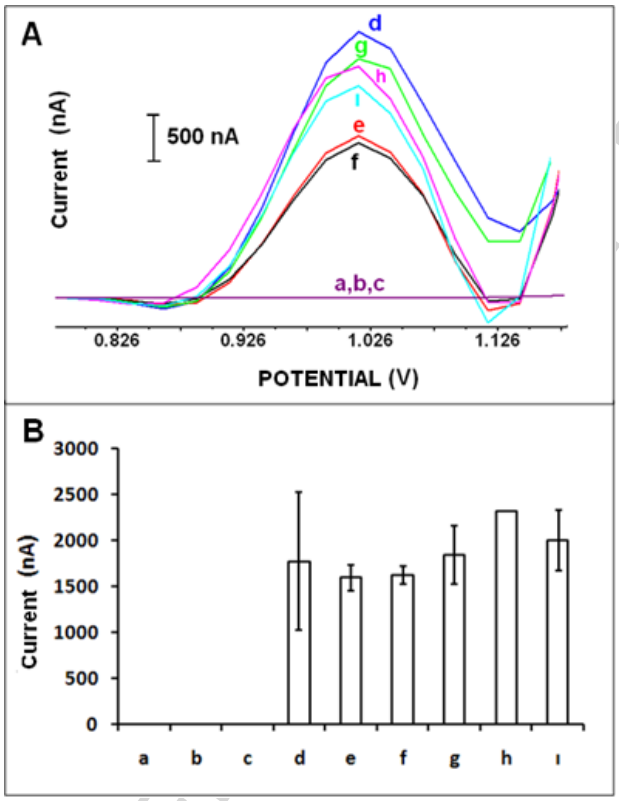

Fig. 6. (A) DPVs, **(B)** histograms representing the control experiment with **(a)** unmodified PGE, **(b)** CA/PGE, **(c)** CA/GO/PGE in ABS, the guanine oxidation signal by 5 µg/mL miRNA-34a G DNA probe immobilized **(d)** CA/PGE**, (e)** CA/GO/PGE, 10 µg/mL miRNA-34a G DNA probe immobilized **(f)** CA/PGE, **(g)** CA/GO/PGE, 15 µg/mL miRNA-34a G DNA probe immobilized **(h)** CA/PGE, **(i)** CA/GO/PGE.

Next, the effect of immobilization time of miRNA-34a G DNA probe from 5 min to 90 min upon to biosensor response investigated and the results were shown in Fig. 7. After miRNA-34a probe immobilization onto electrode surface, there was an increase at guanine signal till 60 min and then it

decreased. The average guanine signal was measured as 2135 ± 89.8 nA (RSD% = 4.2%, n = 4) after the immobilization of 10 µg/mL miRNA-34a at CA/GO/PGEs for 60 min. (Fig. 7A-f).

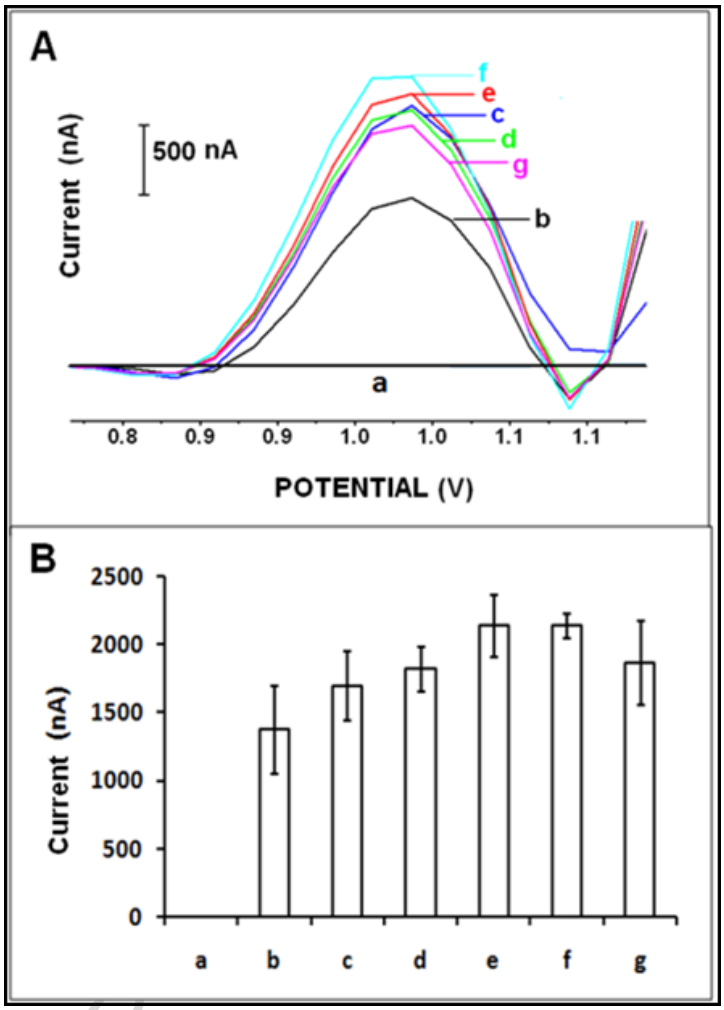

Fig. 7. (A) DPVs, **(B)** histograms representing the guanine oxidation signal of **(a)** CA/GO/PGE in the absence of miRNA-34a G probe, after immobilization of 10 µg/mL miRNA-34a G probe during **(b)** 5 min **(c)** 15 min, **(d)** 30 min, **(e)** 45 min, **(f)** 60 min, (**g)** 90 min onto the surface of CA/GO/PGE (n=3).

The effect of hybridization time between 10 µg/mL inosine substituted miRNA-34a probe and 20 µg/mL miRNA-34a target was explored upon the changes at guanine signal obtained at +1.00 V in the presence of hybridization at surface of CA/GO/PGE (Fig. 8). The average guanine signal of miRNA hybridization observed in various hybridization times; 15 min, 30 min and 60 min was found about

216 ± 29.3 nA (RSD% = 13.6%), 563 ± 172.9 nA (RSD% = 30.7%) and 609 ± 43.1 nA (RSD% = 7.1%), respectively. Even though there was not a critical difference between the responses obtained at 30 min and 60 min hybridization time, more reproducible guanine signal was obtained at 60 min hybridization time. Therefore, 60 min hybridization time was chosen as optimum.

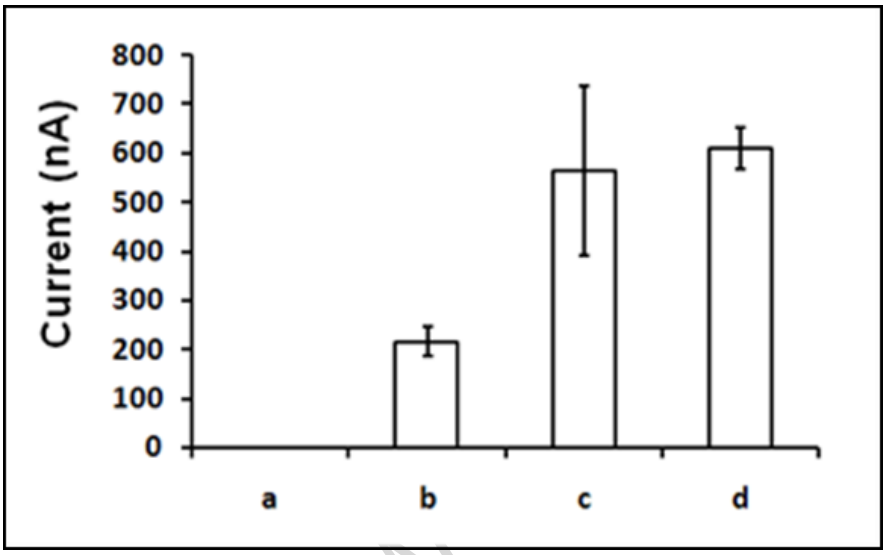

Fig. 8. Histogram representing the average guanine signal of **(a)** 10 µg/mL miRNA-34a I probe immobilized CA/GO/PGE, after hybridization between10 µg/mL miRNA-34a I probe and 20 µg/mL target miRNA-34a during **(b)** 15 min, **(c)** 30 min, **(d)** 60 min (n=3).

Next, the effect of miRNA-34a target concentration upon to biosensor response obtained after full match hybridization occured between 10 µg/mL miRNA-34a I DNA probe and its target RNA at different concentration level from 5 to 40 µg/mL was investigated (Fig. 9). The guanine signal increased until 35 µg/mL miRNA-34a target concentration, then it decreased in the presence of 40 µg/mL target. The detection limit (DL) was calculated in the linear concentration range from 5 to 35 µg/mL (Fig. 9, inset) and it was found to be 7.52 µg/mL (42.7 pmol in 40 µL sample) with a regression equation y = 30.42 x + 70.78 with the coefficient of determination (R^2) of 0.93 according to

the procedure described by Miller and Miller [54]. Since the highest and more reproducible guanine signal was obtained in the presence of hybridization of 10 µg/mL miRNA-34a I probe with 35 µg/mL miRNA-34a target, 35 µg/mL target concentration level was chosen as the optimum one furtherly for selectivity studies.

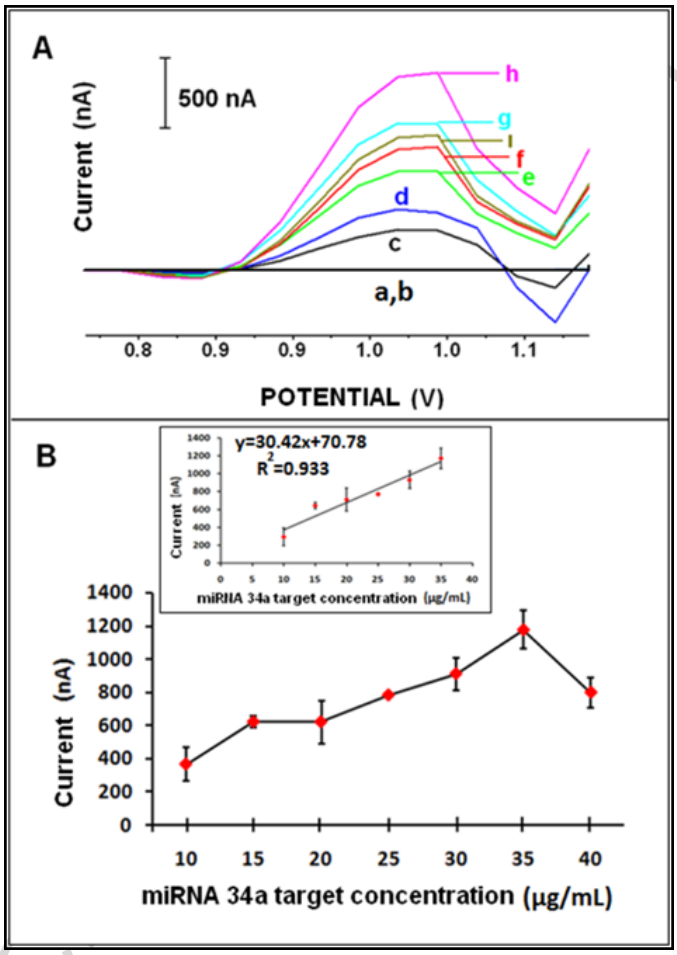

Fig. 9. (A) DPVs **(B)** Line graph representing the guanine signal of **(a)** 10 µg/mL miRNA-34a inosine probe immobilized CA/GO/PGE, after hybridization between 10 µg/mL miRNA-34a I probe and **(b)** 5 µg/mL, **(c)** 10 µg/mL, **(d)** 15 µg/mL, **(e)** 20 µg/mL, **(f)** 25 µg/mL**, (g)** 30 µg/mL**, (h)** 35 µg/mL, **(ı)** 40 µg/mL target miRNA-34a. Inset figure: Calibration plot obtained from guanine oxidation signals after hybridization of miRNA-34a I probe with various concentrations of target miRNA-34a at the surface of CA/GO/PGE.

Under the optimum probe and target values (10 µg/mL and 35 µg/mL, respectively), the optimization of hybridization time was repeated (Fig. 10). The average guanine signal was measured as 1174 ± 115.7 nA (RSD % = 9.8 %) when hybridization was performed during 60 min.

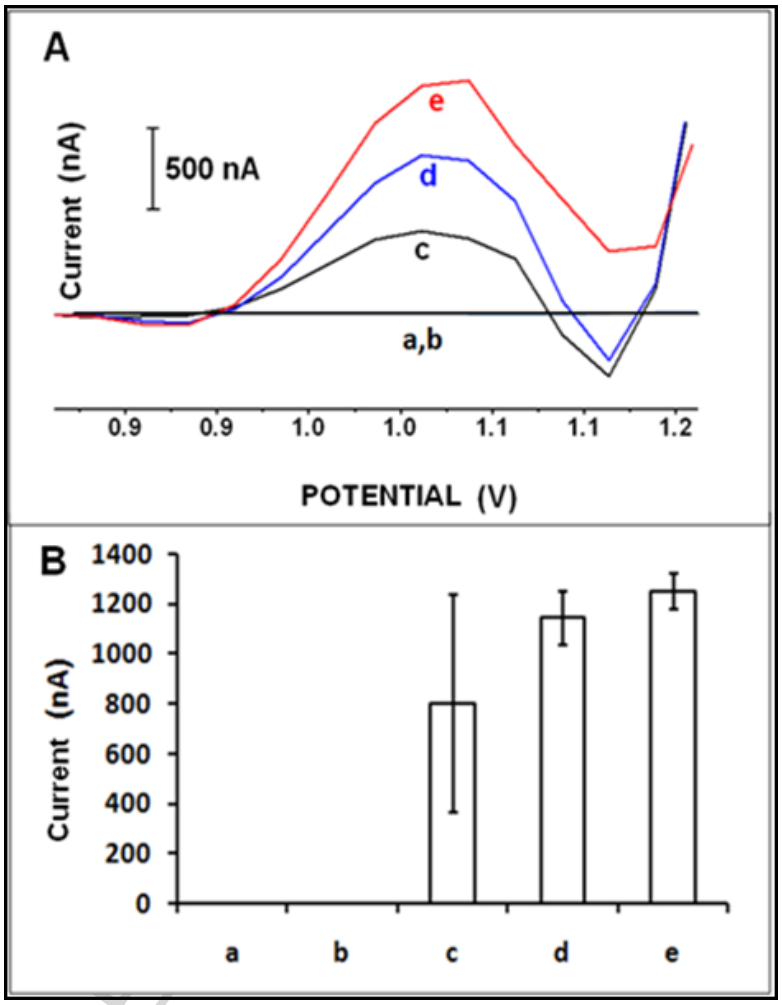

Fig. 10. (A) DPVs **(B)** histograms representing **(a)** the control experiment with CA/GO/PGE in ABS, the guanine signal of **(b)** 10 µg/mL miRNA-34a I probe immobilized CA/GO/PGE, hybridization of 10 µg/mL miRNA-34a I probe with 35 µg/mL target miRNA-34a **(c)** 15 min, **(d)** 30 min, **(e)** 60 min.

The intra-day repeatibility of the results based on miRNA-34a hybridization obtained by CA-GO-PGEs was varying from 8.05 % to 12.84 % consecutively during four days. In order to examine the inter-day reproducibility, these results were combined. Accordingly, the average guanine oxidation signal obtained in the presence of miRNA hybridization was calculated and it was found to be 1301.64 ± 323.22 nA with the RSD % of 24.83 % (n=12).

The selectivity of the electrochemical RNA biosensor developed by CA/GO/PGEs was tested in the presence of 10 µg/mL miRNA-34a I probe and 35 µg/mL target miRNA-34a, miRNA-16, miRNA-155, miRNA-15a, miRNA-660 and the mixture of miRNA-34a : miRNA-16, miRNA-34a : miRNA-155, miRNA-34a : miRNA-15a, miRNA-34a : miRNA-660 (1:1) (Fig. 11). After the hybridization of 10 µg/mL miRNA-34a probe with 35 µg/mL miRNA-34a, miRNA-16, miRNA-155, miRNA-15a, miRNA-660 target, the average guanine signals were measured as 1301.6 ± 323.2 nA, 1194.8 ± 101.5 nA, 316 ± 105.9 nA, 571 ± 159.9 nA and 997.6 ± 300.3 nA with the RSDs % as 24.8 %, 8.5 % , 33.5 %, 28 % and 30.1 %, respectively. Herein, miRNA biosensor based on CA/GO/PGEs presented a very selective behavior to its target miRNA sequence. In the presence of the mixture of miRNA-34a : miRNA-16, miRNA-34a : miRNA-155, miRNA-34a : miRNA-15a, miRNA-34a : miRNA-660, the average guanine signals were measured as 1973.2 ± 852.3 nA, 769.5 ± 869.7 nA, 1093.9 ± 575.2 nA, 1389.5 ± 841.8 nA with the RSDs % as 43.2 %, 113 %, 52.6 %, 60.6 %, respectively (n=3). It could be concluded that our voltammetric biosensor based on CA/GO/PGE presented a selective behavior even in the presence of the mixture sample containing target miRNA-34a besides unwanted substituents; such as, different miRNAs.

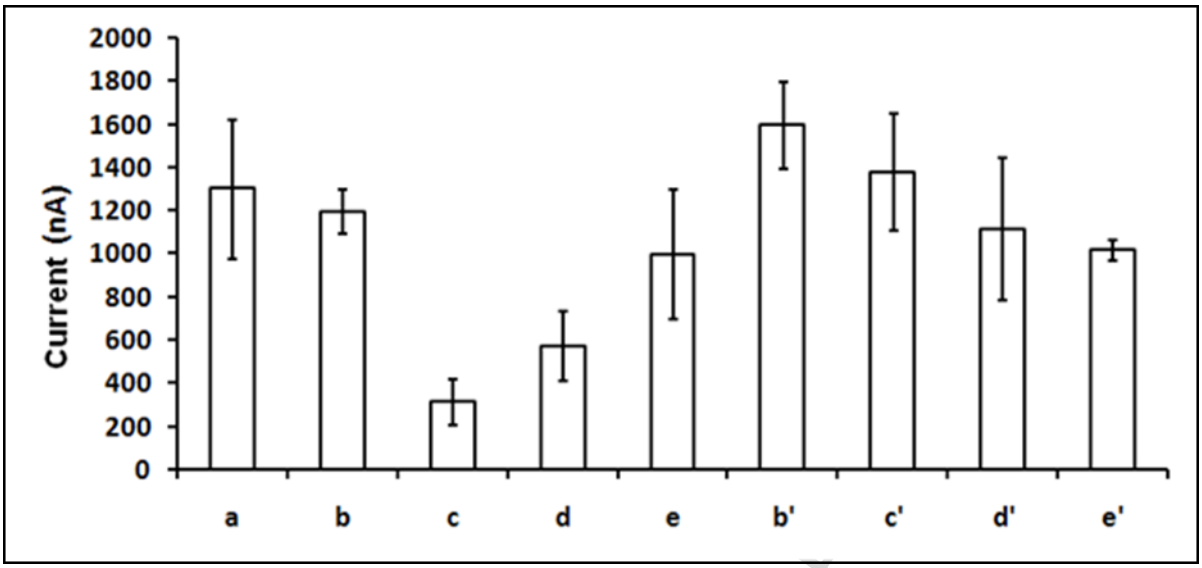

Fig. 11. Histogram representing the average oxidation signal of guanine after hybridization between 10 µg/mL miRNA-34a I probe with 35 µg/mL target **(a)** miRNA-34a **(b)** miRNA-16, **(c)** miRNA-155, **(d)** miRNA-15a, **(e)** miRNA-660, the mixture that contains **(b')** miRNA-34a and miRNA-16, **(c')** miRNA-34a and miRNA-155**, (d')** miRNA-34a and miRNA-15a, **(e')** miRNA-34a and miRNA-660.

4. Conclusions

The present work is the first study in the literature, which introduced the label free voltammetric detection of miRNA-34a by using CA/GO modified PGEs since the modification of graphene oxide (GO) onto the surfaces of chemically activated pencil graphite electrodes (PGEs) was firstly performed herein. These CA/GO modified PGEs were then applied on voltammetric monitoring of miRNAs based on the changes at guanine oxidation signal.

The microscopic and electrochemical characterizations were done using CA/GO/PGEs in contrast to unmodified PGEs via microscopic (SEM) and electrochemical (CV and EIS) techniques. Under the optimum experimental conditions, the selectivity of our electrochemical biosensor was tested. In comparison to the procedure of our previous work [25], the immobilization of GO was performed

herein more effiently due to using chemically activated pencil graphite electrodes (PGEs) by CA agents, EDC/NHS. Accordingly, the binding of DNA-miRNA hybrid onto CA/GO modified PGEs was occured properly. Thus, it resulted with a faster voltammetric detection of miRNA hybridization using DPV technique approximately 1 min, which was 10 times lower than the measurument time (i.e, 10 min) presented earlier study [25].

The PGEs brought also some of crucial advantages herein; such as, being disposable (single-use), easy to use, time saving (i.e., whole procedure including preparation of CA/GO/PGEs and DNA-miRNA hybridization and measurement was resulted in 3 h and 20 min), requiring less chemicals and experimental steps in comparison to the conventional electrodes used for development of graphene based nanomaterials modified biosensors [5,6, 8, 10, 55].

Moreover, a low detection limit was obtained for miRNA-34a target by using CA/GO/PGEs in a faster measurument protocol (i.e 1 min). This is the first study in the literature which evaluated the label free voltammetric detection of miRNA-34a sequence by using CA/GO modified PGEs.

As a conclusion, the CA/GO modified PGEs have been furtherly adapted to the miniaturized novel systems designed for electrochemical detection of nucleic acids, drugs, or, proteins.

Acknowledgements

A.E acknowledges the financial support from Turkish Scientific and Technological Research Council (TÜBİTAK) (Project No.115Z099) and Ege University Scientific Research Project Coordination (Project no.16/FBE/011) as the Project Investigator of these projects, and she also would like to express her gratitude to the Turkish Academy of Sciences (TUBA) as an Principal member for its partial support. D.I acknowledges a master project scholarship by TÜBİTAK (Project No.115Z099).

References

[1] A.K. Geim, K.S. Novosolov, The rise of graphene, Nature Materials 6 (2007) 183-191.

[2] M. Hassan, E. Haque, K.R. Reddy, A.I. Minett, J. Chen, V.G. Gomes, Edge-enriched graphene quantum dots for enhanced photo-luminescence and supercapacitance, Nanoscale 6 (2014) 11988-11994.

]3] J. Kotakoski, C. Brand, Y. Lilach, O. Cheshnovsky, C. Mangler, M. Arndt, J. C. Meyer, Toward two-dimensional all-carbon heterostructures via ion beam patterning of single-layer graphene, Nano Lett. 15 (2015) 5944-5949.

[4] H. Dong, Z. Zhu, H. Ju, F. Yan, Triplex signal amplification for electrochemical DNA biosensing by coupling probe-gold nanoparticles-graphene modified electrode with enzyme functionalized carbon sphere as tracer, Biosens. Bioelectron. 33 (2012) 228-232.

[5] S.Alwarappan, A. Erdem, C. Liu, C.Z. Li., Probing the electrochemical properties of graphene nanosheets for biosensing applications, J Phys. Chem. C 113 (2009) 8853–8857.

[6] S. Hajihosseini, N. Nasirizadeh, M.S. Hejazi, P. Yaghmaei, A sensitive DNA biosensor fabricated from gold nanoparticles and graphene oxide on a glassy carbon electrode, Mater. Sci Eng. C 61 (2016) 506-515.

[7] M. Hassan, K.R. Reddy, E. Haque, A.I. Minett, V.G. Gomes, High-yield aqueous phase exfoliation of graphene for facile nanocomposite synthesis via emulsion polymerization, Journal of Coll. and Int. Sci. 410 (2013) 43-51.

[8] C. Xue, X. Wang, W. Zhu, Q. Han, C. Zhu, J. Hong, X. Zhou, H. Jian, Electrochemical serotonin sensing interface based on double-layered membrane of reduced graphene oxide/polyaniline nanocomposites and molecularly imprinted polymers embedded with gold nanoparticles, Sens. Act. B 196 (2014) 57–63.

[9] A. Erdem, E. Eksin, M. Muti, in: M. Aliofkhazraei, N. Ali, W.I. Milne, C.S. Ozkan, S. Mitura, J.L. Gervasoni (Eds.), Graphene-based biosensor technologies, Graphene Science Handbook, CCR Press, 2016, pp.93-105.

[10] G. Yang, J. Cao, L. Li, R.K. Rana, J.J. Zhu, Carboxymethyl chitosan-functionalized graphene for label-free electrochemical cytosensing, Carbon 51 (2013) 124-133.

[11] T. Yang, L. Meng, X. Wang, X, Wang, L. Wang, K. Jiao, Direct electrochemical DNA detection originated from the self-redox signal of sulfonated polyaniline enhanced by graphene oxide in neutral solution, ACS Appl. Mater. Interfaces 5 (2013) 10889-10894.

[12] A. Erdem, E. Eksin, M. Muti, Chitosan-graphene oxide based aptasensor for the impedimetric detection of lysozyme, Colloid. Surf. B 115 (2014) 205-211.

[13] S. Ray, Applications of Graphene and Graphene-Oxide Based Nanomaterials, chapter 2: Application and uses of graphene oxide and reduced graphene oxide, Elsevier, Oxford, 2015, pp. 39-55.

[14] X. Li, W. Cheng, D. Li, J. Wu, X. Ding, Q. Cheng, S. Ding, A novel surface plasmon resonance biosensor for enzyme-free and highly sensitive detection of microRNA based on multi component nucleic acid enzyme (MNAzyme)-mediated catalyzed hairpin assembly, Biosens. and Bioelectron. 80 (2016) 98-104.

[15] Y. Xu, Y. Wang, S. Liu, J. Yu, H. Wang, Y. Guo, J. Huang, Ultrasensitive and rapid detection of miRNA with three-way junction structure-based trigger-assisted exponential enzymatic amplification, Biosens. Bioelectron. 81 (2016) 236-241.

[16] A.W. Wark, H. J. Lee, R.M. Corn, Multiplexed detection methods for profiling microRNA expression in biological samples, Angew. Chem. Int. Ed. 47 (2008) 644-652.

[17] B.D. Adams, C. Parsons, F. J. Slack, The tumor-suppressive and potential therapeutic functions of miR-34a in epithelial carcinomas, Journal Expert Opinion on Therapeutic Targets 20 (2016) 737-753.

[18] K.A. Cissel, S.K. Deo, Trends in microRNA detection, Anal. Bioanal. Chem. 394 (2009) 1109-1116.

[19] J. Koshiol, E. Wang, Y. Zhao, F. Marincola, M.T. Landi, Strengths and limitations of laboratory procedures for microRNA detection, Cancer Epidemiol. Biomark. Prev. 19 (2010) 907–911.

[20] Y.Y. Yu, Z.G. Chen, L.J. Shi, F. Yang, J.B. Pan, B.B. Zhang, D.P. Sun, Ultrasensitive electrochemical detection of microRNA based on an arched probe mediated isothermal exponential amplification, Anal. Chem. 86 (2014) 8200–8205.

[21] A.R. Cardoso, F. T.C. Moreiraa, R. Fernandes, M. G.F. Sales, Novel and simple electrochemical biosensor monitoring attomolar levels of miRNA-155 in breast cancer, Biosens. Bioelectron 80 (2016) 621–630.

[22] A. Erdem, G. Congur, E. Eksin, Multi channel screen printed array of electrodes for enzyme-linked voltammetric detection of MicroRNAs, Sens. Act. B 188 (2013) 188 1089-1095.

[23] A. Erdem, G. Congur, Label-free voltammetric detection of MicroRNAs at multi-channel screen printed array of electrodes comparison to graphite sensors, Talanta 118 (2014) 7-13.

[24] T. Kilic, A. Erdem, Y. Erac, M. O. Seydibeyoglu, S. Okur, M. Ozsoz, Electrochemical Detection of a Cancer Biomarker mir-21 in Cell Lysates Using Graphene Modified Sensors, Electroanalysis 27 (2015) 317-326.

[25] G. Congur, E. Eksin, A. Erdem, Impedimetric detection of microRNA at graphene oxide modified sensors, Electrochim. Acta 172 (2015) 20–27.

[26] T. Kilic, M. Kaplan, S. Demiroglu, A. Erdem M. Ozsoz, Label-free electrochemical detection of microRNA-122 in real samples by graphene modified disposable electrodes, J. Electrochem. Soc. 163 (2016) B227-B233.

[27] S. Babapoor, M. Horwich, R. Wu, S. Levinson, M. Gandhi, H. Makkar, A. Kristjansson, M. Chang, S.S Dadras, microRNA in situ hybridization for miR-211 detection as an ancillary test in melanoma diagnosis, Modern Pathology 29 (2016) 461-475.

[28] P. Zhang, X. Wu, R. Yuan, Y. Chai, An "Off-On" Electrochemiluminescent biosensor based on DNAzyme-assisted target recycling and rolling circle amplifications for ultrasensitive detection of microRNA, Anal. Chem. 87 (2015) 3202-3207.

[29] X. Qiu, X. Liu, W. Zhang, H. Zhang, T. Jiang, D. Fan, Y. Luo, Dynamic monitoring of MicroRNA-DNA hybridization using DNAase-triggered signal amplification, Anal. Chem. 87 (2015) 6303-6310.

[30] W. Ma, B. Situ, W. Lv, B. Li, X. Yin, P. Vadgama, L. Zheng, W. Wang, Electrochemical determination of microRNAs based on isothermal strand-displacement polymerase reaction coupled with multienzyme functionalized magnetic micro-carriers, Biosens. Bioelectron. 80 (2016) 344–351.

[31] S. Campuzano, M. Pedrero, J.M. Pingarrón, Electrochemical genosensors for the detection of cancer-related miRNAs, Anal. Bioanal. Chem. 406 (2014) 27-33.

[32] E. Hamidi-Asl, I. Palchetti, E. Hasheminejad, M. Mascini, A review on the electrochemical biosensors for determination of microRNAs, Talanta 115 (2013) 74-83.

[33] M. Bartosik, R. Hrtska, E. Palecek, B. Vojtesek, Magnetic bead-based hybridization assay for electrochemical detection of microRNA, Anal. Chim. Acta 813 (2014) 35-40.

[34] H. Yin, Y. Zhou, H. Zhang, X. Meng, S. Ai, Electrochemical determination of microRNA-21 based on graphene, LNA integrated molecular beacon, AuNPs and biotin multifunctional bio bar codes and enzymatic assay system, Biosens. Bioelectron. 33 (2012) 247-253.

[35] Y. Wen, G. Liu, H. Pei, L. Li, Q. Xu, W. Liang, Y. Li, L. Xu, S. Ren, C. Fan, DNA nanostructure-based ultrasensitive electrochemical microRNA biosensor, Methods 64 (2013) 276-282.

[36] H.V. Tran, B. Piro, S. Reisberg, L.D. Tran, H.T. Duc, M.C. Pham, Label-free and reagentless electrochemical detection of microRNAs using a conducting polymer nanostructured by carbon nanotubes: Application to prostate cancer biomarker miR-141, Biosens. Bioelectron. 49 (2013) 164-169.

[37] E. Sun, L. Wang, X Zhou, C. Ma, Y. Sun, M. Lei, B. Lu, R. Han, Graphene oxide/DNA-decorated electrode for the fabrication of microRNA biosensor, Roy. Soc. Chem. 5 (2015) 69334-69339.

[38] S.R. Ryoo, J. Lee, J. Yeo, H.K. Na, Y.K. Kim, H. Jang, J.H. Lee, S.W. Han, Y. Lee, V.N. Kim, D.H. Min, Quantitative and multiplexed microRNA sensing in living cells based on peptide nucleic acid and nano graphene oxide (PANGO), J. Am. Chem. Soc. 7 (2013) 5882-5891.

[39] Y. Ren, H. Deng, W. Shen, Z. Gao, A highly sensitive and selective electrochemical biosensor for direct detection of microRNAs in serum, Anal. Chem. 85 (2013) 4784-4789.

[40] X. Meng, Y. Zhou, Q. Liang, X. Qu, Q. Yang, H. Yin, S. Ai, Electrochemical determination of microRNA-21 based on bio bar code and hemin/G-quadruplet DNAenzyme, Analyst 138 (2013) 3409-3415.

[41] M. Labib, N. Khan, S.M. Ghobadloo, J. Cheng, J.P. Pezacki, M.V. Berezovski, Three-mode electrochemical sensing of ultralow microRNA levels, J. Am. Chem. Soc. 135 (2013) 3027-3038.

[42] Z. Gao, H. Deng, W. Shen, Y. Ren, A label-free biosensor for electrochemical detection of femtomolar microRNAs, Anal. Chem. 85 (2013) 1624-1630.

[43] F.F. Cheng, J.J Zhang, T.T. He, J.J. Shi, E.S. Abdel-Halimc, J.J Zhu, Bimetallic Pd-Pt supported graphene promoted enzymatic redox cycling for ultrasensitive electrochemical quantification of microRNA from cell lysates, Analyst 139 (2014) 3860-3865.

[44] M. Bartosik, M. Trefulka, R. Hrstka, B. Vojtesek, E. Palecek, Os(VI)bipy-based electrochemical assay for detection of specific microRNAs as potential cancer biomarkers, Electrochem. Comm. 33 (2013) 55-58.

[45] S. Sam, L. Touahir, J. S. Andresa, P. Allongue, J. N. Chazalviel, A. C. Gouget-Laemmel, C. H. Villeneuve, A. Moraillon, F. Ozanam, N. Gabouze, S. Djebbar, Semiquantitative study of the EDC/NHS activation of acid terminal groups at modified porous silicon surfaces, Langmuir 26 (2010) 809–814.

[46] E. Eksin, A. Erdem, Chitosan-carbon nanofiber modified single-use graphite electrodes developed for electrochemical detection of DNA hybridization related to Hepatitis B virus, Electroanalysis 28 (2016) 2514-2521.

[47] E. A. Lusi, M.Passamano, P.Guarascio, A.Scarpa, L.Schiavo, Innovative electrochemical approach for an early detection of microRNAs, Anal. Chem. 81 (2009) 2819–2822.

[48] N. Shang, P. Papakonstantinou, M. McMullan, M. Chu, A. Stamboulis, A. Potenza, S. S. Dhesi and H. Marchetto, Catalyst-Free efficient growth, orientation and biosensing properties of multilayer graphene nanoflake films with sharp edge planes, Adv. Funct. Mater. 18 (2008) 3506–3514.

[49] F. Yang, K. J. Huang, D. J. Niu, C. P. Yang and Q. S. Jing, TiO2-graphene nanocomposite for electrochemical sensing of adenine and guanine, Electrochim. Acta 56 (2011) 4685–4690.

[50] X. Qi, H. Gao, Y. Zhang, X. Wang, W. Sun, Electrochemical DNA biosensor with chitosan-Co_3O_4 nanorod-graphene composite for the sensitive detection of staphylococcus aureus nuc gene sequence, Bioelectrochemistry 88 (2012) 42–47.

[51] M.M. Barsan, K. P. Prathish, X. Sun, C.M.A Brett Nitrogen doped graphene and its derivatives as sensors and efficient direct electron transfer platform for enzyme biosensors, Sens Act B 203 (2014) 579-587.

[52] T.E. Cummings, P.J. Elving Determination of the electrochemically effective electrode area, Anal Chem 50 (1978) 480-488.

[53] W. Sun, Y. Lu, Y. Wu, Y. Zhang, P. Wang, Y. Chen, G. Li, Electrochemical sensor for transgenic maize MON810 sequence with electrostatic adsorption DNA on electrochemical reduced graphene modified electrode, Sens Act B 202 (2014) 160-166.

[54] J. N. Miller, J. C. Miller, Statistics and chemometrics for analytical chemistry, Pearson Education, Essex, UK, 2005, pp. 121–123.

[55] Y. R. Kim, S. Bong, Y. J. Kang, Y. Yang, R. K. Mahajan, J. S. Kim, H. Kim, Electrochemical detection of dopamine in the presence of ascorbic acid using graphene modified electrodes, Biosens. Bioelectron. 25 (2010) 2366–2369.

Highlights:

- Graphene oxide modified electrodes were used for voltammetric detection of miRNA
- The characterization of CA-GO-PGEs was performed by SEM and cyclic voltammetry
- Voltammetric detection of miRNA-34a was performed by differential pulse voltammetry
- miRNA-34a spesific biosensor presented good selectivity towards to other miRNAs

Graphical abstract: